Species and tissue specific differences in ROS metabolism to hypoxia- and hyperoxia-recovery exposure in marine sculpins

G.Y. Lau[1], S. Arndt[2], M.P. Murphy[2], and J.G. Richards[1]

[1]Department of Zoology, University of British Columbia, 6270 University Blvd, Vancouver, BC, V6T 1Z4, Canada

[2]MRC Mitochondrial Biology Unit, University of Cambridge, Hills Road, Cambridge, CB2 0XY, United Kingdom

Corresponding author: G.Y. Lau (glau@zoology.ubc.ca)

Abstract

Animals that inhabit environments that fluctuate in oxygen must not only contend with disruptions to aerobic metabolism, but also the potential effects of reactive oxygen species (ROS) generation. The goal of this study was to compare aspects of ROS metabolism in response to O_2 variability (6 hr hypoxia or hyperoxia, with subsequent normoxic recovery) in two species of intertidal sculpin fishes (Cottidae, Actinopterygii) that can experience O_2 fluctuations in their natural environment and differ in whole animal hypoxia tolerance. To assess ROS metabolism, we measured the ratio of glutathione and glutathione disulfide as an indicator of tissue redox environment, MitoP/MitoB ratio to assess *in vivo* mitochondrial ROS generation, thiobarbituric acid reactive substances (TBARS) for lipid peroxidation, and total oxidative scavenging capacity (TOSC) in the liver, brain, and gill. In the brain, the more hypoxia tolerant *O. maculosus* showed large increases in TBARS levels following hypoxia and hyperoxia exposure that were generally not associated with large changes in mitochondrial H_2O_2. In contrast, the less-tolerant *S. marmoratus* showed no significant changes in TBARS or mitochondrial H_2O_2 in the brain. More moderate responses were observed in the liver and gill of *O. maculosus* exposed to hypoxia and hyperoxia with normoxic recovery, whereas *S. marmoratus* showed more responses to O_2 variability in these tissues. Our results show that the relationship between hypoxia tolerance and ROS metabolism is species and tissue specific.

Introduction

The majority of reactive oxygen species (ROS) are generated at sites along the mitochondrial electron transport system (ETS) and the rate of ROS generation is dependent upon the interactive effects of mitochondrial activity, proton motive force, ETS reduction/oxidation (redox) state, and O_2 availability (Quinlan et al., 2013). Mitochondria continuously produce ROS at low rates for cell signaling (D'Autréaux and Toledano, 2007), but ROS generation can increase when ETS flux is low, redox environment in mitochondria is highly reduced, and proton motive force is high (Brand, 2000; Niknahad et al., 1995). ROS generation also increases when O_2 availability is high, *e.g.* during normoxic recovery after hypoxia or during hyperoxia, when the redox environment in mitochondria is relatively oxidized (Aon et al., 2010; Yusa et al., 1987). High rates of mitochondrial ROS production can overwhelm total cellular scavenging capacities, resulting in oxidative damage to DNA, proteins, and lipids (Cadet, 2003; Gutteridge, 1995; Reznick and Packer, 1994). In most vertebrates, particularly mammals, high rates of ROS production and the associated tissue damage typically occurs during periods of O_2 fluctuation such as those associated with ischemia-reperfusion injury (Chouchani et al., 2014).

Animals that inhabit environments that naturally fluctuate in O_2, particularly those that experience hypoxia, often display adaptations that enhance whole-animal O_2 uptake and use under O_2 limiting conditions, so as to sustain aerobic metabolism (Scott et al., 2009; Storz et al., 2009). In contrast, much less is known about whether animals that inhabit these environments have also evolved strategies to minimize ROS production or mitigate the damaging effects of ROS. Several studies support the idea that hypoxia tolerance is associated with lowered mitochondrial ROS generation (shown in elasmobranchs, molluscs, and hypoxia-acclimated killifish *Fundulus heterolitus*; Du et al., 2016; Hickey et al., 2012; Ivanina and Sokolova, 2016), whereas there does not appear to be a consistent link between hypoxia tolerance and antioxidant defenses in fish (Leveelahti et al., 2014). However, a previous *in vitro* study of brain mitochondria from multiple species of intertidal sculpin (Cottidae, Actinopterygii) showed that mitochondria from more hypoxia tolerant species emitted higher H_2O_2 per O_2 consumed under oligomycin-induced state IV conditions compared to a less hypoxia tolerant species, and H_2O_2 emitted per mg mitochondrial protein measured did not differ (Lau and Richards 2019). Together, these *in vitro* studies suggest that at the level of the mitochondria, the relationship between hypoxia tolerance and ROS metabolism is nuanced, possibly due to variation in the role of ROS in cell signaling and the role of mitochondria as regulators of ROS metabolism *in vivo* (Munro and Treberg, 2017). Thus, the goal of this study was to determine if *in vivo* ROS metabolism differs between two species of sculpin, *Oligocottus maculosus* and *Scorpaenichthys marmoratus,* that vary in

hypoxia tolerance and experience different O_2 regimes in their natural environment. *O. maculosus* resides predominately in rock pools in the marine intertidal zone, where O_2 can fluctuate daily from near anoxia to hyperoxia (Richards, 2011), whereas *S. marmoratus* primarily inhabits the subtidal environment, which is near normoxia and far more O_2 stable. Previous work has demonstrated that *O. maculosus* is far more hypoxia tolerant than *S. marmoratus* and they differ in brain mitochondrial function, but not tissue mitochondrial content (Lau and Richards, 2018; Lau et al., 2017; Mandic et al., 2009a).

In order to manipulate and gain insight into how ROS metabolism differs between hypoxia tolerant and intolerant fish, each species of sculpins was exposed to hypoxia (3.5 kPa O_2) or hyperoxia (64 kPa O_2) for 6 hr, with or without 1 hr recovery in normoxic water. These exposure times and PO_2 levels mimic those observed in the marine intertidal zone (Richards, 2011). Following O_2 manipulations, *in vivo* ROS metabolism was assessed in liver, gill, and brain. Tissue redox status was assessed as the relative ratio of glutathione (GSH) and glutathione disulfide (GSSH), which is one of the dominant redox couples within the cell (Rahman et al., 2006). To estimate *in vivo* mitochondrial H_2O_2 production, we used the ratiometric mitochondria-targeted mass spectrometry probe MitoB, which is phenylboronic acid conjugated to a triphenylphosphonium ion (TPP^+; Cochemé et al., 2011; Logan et al., 2014). MitoB can be injected into an animal where it accumulates in the mitochondrial matrix where it reacts with H_2O_2 to form a stable phenol product, MitoP, which can be assessed in tissue samples *via* mass spectrometry. To gain insight into the effects of our O_2 manipulations on oxidative damage, we assessed lipid peroxidation by measuring thiobarbuturic acid reactive substances (TBARS) levels (Gutteridge, 1995). We also assessed tissue total oxidative scavenging capacity (TOSC). We hypothesized that the more hypoxia tolerant sculpin, *O. maculosus*, would be more resistant to changes in environmental O_2 and show less disturbance of *in vivo* ROS metabolism as compared with the less tolerant sculpin, *S. marmoratus*.

Methods

Chemicals

MitoB compounds used for this study were synthesized by Prof. Richard Hartley (University of Glasgow). The details of the synthesis of MitoB and associated compounds are described in (Cochemé et al., 2011). Chemicals for biochemical analysis were purchased from Sigma-Aldrich unless otherwise specified.

Animals

Adult *O. maculosus* (average 3.95 ± 0.17 g) and *S. marmoratus* (average 21.71 ± 1.64 g) were collected near Bamfield Marine Sciences Centre (British Columbia, Canada) at Ross Islets (48°52.4'N, 125°9.7'W) and Wizard's Rock (48°51.5'N, 125°9.4'W) using either handheld nets or pole seines during the lowest point in the tidal cycle. Animals were transported to The University of British Columbia (UBC) and housed in a recirculating aquaculture system (RAS) with artificial seawater at 12 °C and maintained on a diet of shrimp, Atlantic krill, and bloodworms for at least 3 weeks before experimentation. All experimental procedures were reviewed and approved by the UBC Animal Care Committee under animal use protocol number A13-0309.

Validation of MitoB use in sculpins

Individual *O. maculosus* were retrieved from stock RAS tanks and injected intraperitoneally with 30 nmol of MitoB (50 µL injection volume in phosphate-buffered saline containing a small amount of food coloring to facilitate visibility) using a BD Ultra-Fine™ syringe (6 mm needle). Following injection, fish were transferred to separate 1.1 L plastic mesh baskets (with three fish each) and held in a wet table with recirculating seawater at 12 °C. At 0.5, 1, 4, 8, 24, and 72 hrs post-injection, three animals were removed from the mesh baskets, anaesthetized with 0.5 g/L benzocaine, and gills, brain, muscle, and liver were dissected, frozen in liquid nitrogen, and stored at -80 °C until processing (see below).

To further validate whether MitoB behaves similarly in marine teleosts as in murine models (Cochemé et al., 2011), we used an ion-selective electrode for TPP^+ to monitor the uptake of MitoB into isolated liver mitochondria (see Lau et al. 2017 for isolation protocol) from another species of marine sculpin, *Artedius lateralis* (Supplementary Fig.1). After MitoB titrations, the addition of NADH-generating substrates for complex I (5 mM pyruvate, 10 mM malate, and 10 mM glutamate) and 10 mM succinate for complex II substrate to stimulate state II respiration rate led to a decrease in MitoB detected in the extra-mitochondrial surroundings, indicating an influx of MitoB into the matrix (Supplementary Fig.1). The addition of 0.5 µM of the uncoupler carbonyl cyanide 4-(trifluoromethoxy)phenylhydrazone (FCCP) caused an increase in MitoB detected in the extra-mitochondrial surroundings, indicating an efflux of MitoB from matrix.

Experimental protocol and sampling

Both species of sculpin were exposed to one of five treatments after which tissue sampling occurred: 1) 6 hr normoxia, 2) 6 hr hypoxia, 3) 6 hr hypoxia followed by 1 hr normoxic recovery, 4) 6 hr hyperoxia, and 5) 6 hr hyperoxia followed by 1 hr normoxic recovery. For the hypoxia

treatment, both species were exposed to 3.5 kPa, which is at the critical O_2 tension for O_2 consumption rate (P_{crit}) for more hypoxia tolerant *O. maculosus* and is equivalent to exposure to 65% of P_{crit} in the less hypoxia tolerant *S. marmoratus* (Mandic et al., 2009b). Thus, the hypoxia exposure was more severe relative to P_{crit} for *S. marmoratus* than for *O. maculosus*. For hyperoxia treatment, both species were exposed to 64 kPa, which is a PO_2 that is frequently experienced in the higher intertidal and less in the subtidal (Richards 2011).

The treatments were set up in two covered aquaria, one for normoxic control animals and the other for O_2 manipulations (hypoxia and hyperoxia exposures were carried out on two separate days), which were placed in a wet table with recirculating water chilled to 12 °C. Small circulating water pumps inside each aquarium ensured adequate mixing throughout the experiment. To initiate the experiment, individuals of both species were taken from their stock tank and injected intraperitoneally with MitoB (approximately 30 nmol per *O. maculosus* and 60 nmol per *S. marmoratus* in 50 µL of phosphate-buffered saline), yielding ~7.6 and 2.8 nmol/g in the two species, respectively which is within the range used in a previous study on brown trout; Salin et al. 2017) and placed into 1.1 L plastic mesh baskets weighted with gravel (4-6 of *O. maculosus* and 2-3 of *S. marmoratus* in each basket) in the treatment aquaria. Although there are slight differences in the amount of MitoB injected in the two species, these differences have no impact on the study outcomes because both MitoB and MitoP were well-above the detection limit of the mass spectrometer and the ratiometic nature of MitoP/MitoB analysis is insensitive to minor differences in injection amount. One hour after MitoB injection, fish for the first normoxic control timepoint were sampled as described below. The PO_2 of the seawater was then adjusted to the desired level with either nitrogen gas (for hypoxia), 100 % O_2 (for hyperoxia), or aerated with compressed air (normoxia) and maintained at these levels for 6 hrs. Oxygen levels were monitored with a hand-held O_2 probe (Oakton Instruments; for hypoxia) or a FOXY fluorescent O_2 probe (Ocean Optics; for hyperoxia) and O_2 level never deviated from the setpoint by more than 1.5 %. At 6 hr of hypoxia/hyperoxia treatment a total of 12 individuals of *O. maculosus* and 8 individuals of *S. marmoratus* were sampled as described below. Following sampling at 6 hrs, both the hypoxic and hyperoxic aquaria were quickly returned to normoxia (within 30 min) by aeration and a total of 12 individuals of *O. maculosus* and 8 individuals of *S. marmoratus* were sampled at 1 hr recovery once normoxia was established. Paired normoxic controls of 12 individuals of *O. maculosus* and 8 individuals of *S. marmoratus* were also sampled at 6 hrs exposure and 1 hr recovery. For tissue sampling, the mesh basket containing fish was gently moved into a submerged 3.7 L container and both the fish and container were removed from the treatment aquarium and a high dose of anaesthetic (0.5 g/L benzocaine) was introduced to the container.

This procedure ensured that the animals were never exposed to air and that water PO_2 was maintained at the desired level during anaesthesia. We elected to use a high dose of benzocaine to facilitate rapid anaesthesia (within 30 sec). No signs of distress were noted during fish transfer or anaesthesia. Once the fish were unresponsive to touch, they were removed from the anaesthetic bath and brain, gill, and liver were dissected, frozen in liquid N_2, and stored at -80 °C until analyses of MitoB, MitoP, TBARS, GSH/GSSG, and TOSC. Due to the small amount of tissue available, we did not perform all analysis on all tissues sampled from individuals, but instead prioritized analysis of MitoP/MitoB, TBARS, TOSC and performed analysis of GSH/GSSG only on available samples. As a result, some of the n values for GSH/GSSG are low, but still sufficient for basic statistical analysis.

Extraction and purification of MitoP/MitoB

Approximately 30 mg of frozen tissue was homogenized in 210 µL ice-cold 60 % acetonitrile/0.1 % formic acid spiked with internal standards (10 µM d_{15}-MitoB/5 µM d_{15}-MitoP) in the bullet bead homogenizer (Next Advance; New York, USA). Homogenates were centrifuged at 16000 *g* for 10 min at 4 °C, after which the supernatant was transferred to a new 1.5 mL micro-centrifuge tube. The tissue was then resuspended in 200 µL 60 % acetonitrile/0.1 % formic acid, homogenized again, and centrifuged at 16000 *g* for 10 min at 4 °C. The resulting supernatant was combined with the previous supernatant, vortexed for 10 sec, and incubated at 4 °C for 30 min. Samples were then centrifuged at 16000 *g* for 10 min, and the supernatant was filtered with the Millipore centrifugal filter plate (0.45 µm hydrophilic**,** low protein binding Durapore membrane), centrifuged at 3000 *g* for 10 min. The filtrate was collected and the samples were dried in a vacuum speed centrifuge (Labconco Centrivap Concentrator; Kansas City, MO, USA). The dried sample was then resuspended in 250 µL 20 % acetonitrile/0.1 % formic acid, vortexed for 5 min and centrifuged at 16000 *g* for 10 min. 200 µL of the suspension was used for LC-MS/MS analysis. Standard curves for MitoB (0 to 1000 pmol) and MitoP (0 to 1000 pmol) were prepared with salmon tissue. The standards were prepared for analysis with the same procedure as described above (standard curves in Supplementary Fig.2).

LC-MS/MS analysis for MitoP/MitoB

The LC-MS/MS analysis was carried according to the general protocol described elsewhere (Cochemé et al., 2012) with a few modifications. For LC-MS/MS analyses the mass spectrometer was connected in series to an I-class Aquity LC system (Waters). Samples were stored in an autosampler at 4 °C and 2 µL of the sample was injected into a 15 µL flow-through needle and RP-UPLC at 40 °C using an Acquity UPLC® BEH C18 column (1 x 50 mm, 1.7 µm; Waters)

with a Waters UPLC filter (0.2 μm). MS buffers A (95% water/ 5% acetonitrile/ 0.1% formic acid) and B (90% acetonitrile/ 10% water/ 0.1% formic acid) were infused at 200 μL/min using the following gradient: 0-0.3 min, 5% B; 0.3-3 min, 5%-100% B; 3-4 min, 100 % B, 4.0-4.10, 100 %-5 % B; 4.10-4.60 min, 5% B. Eluant was diverted to waste at 0-1 min and 4-4.6 min. The compounds were detected in multiple reactions monitoring in positive ion mode. With this method selected precursor ions are fragmented to product ions, which are used for the precursor ion identification. For quantification, the following transitions were used: MitoB, 397 > 183; d_{15}-MitoB, 412 > 191; MitoP, 369 > 183; d_{15}-MitoP, 384 > 191. The peak area of MitoB, MitoP and internal standard of samples and standard curves were quantified using the MassLynx 4.1 software. The amount of MitoB and MitoP in the samples was determined using the standard curves. The deuterated internal standards were used to normalize samples to account for variation in sample volume.

Tissue glutathione redox potential

Glutathione (GSH) and glutathione disulfide (GSSG) were assayed with the enzymatic recycling method described in Rahman et al. (2006). Briefly, approximately 25 mg of each tissue was homogenized in 180 μL buffer with 0.1 M KH_2PO_4 and 5mM EDTA at pH 7.5 (KPE buffer) with 0.1 % triton X-100 and 0.6 % sulfosalicylic acid. The homogenized sample was then centrifuged at 3000 *g* for 10 min at 4 °C. The supernatant was then divided for assessment of total GSH and GSSG. To determine GSSG, 50 μL of the samples or GSSG standards were incubated for 1 hr at room temperature with 1 μL vinylpyridine (1:10 v/v in KPE buffer) to derivatize GSH. After 1 hr, 3 μL triethanolamine (1:6 in KPE buffer) was added to the samples/standards and they were incubated for 10 min at room temperature, which was followed by the addition of 3 μL 1 M HCl to neutralize the sample. The GSSG and total GSH samples were then assayed using the same protocol in which glutathione reductase (GR) converts GSSG into GSH. For the assay, the buffer was prepared with equal volumes of 1.7 mM [5,5'-dithio-bis(2-nitrobenzoic acid)] (DTNB) and glutathione reductase (3.33 U/mL KPE), of which 125 μL is added to 20 μL of standard/sample. 60 μL of 0.8 mM ß-NADPH was added to start the reaction and the rate of TNB formation was monitored at 412 nm for 5 min. GSH was calculated as the difference between total glutathione and GSSG. At a pH of 7.5 and standard/assay temperature of 25 °C, the standard reduction potential of GSH/GSSG is -270 mV (= -240 mV + [(7.5-7.0) x -59] mV; Schafer and Buettner, 2001). In order to calculate the tissue GSH reduction potential, we used E= -270 mV – 30 x log($[GSH]^2$/[GSSG]), where [GSH] and [GSSG] are the molar concentrations of GSH and GSSG.

Thiobarbuturic acid reactive substances (TBARS)

Tissue TBARS was assessed using a commercially available kit (TBARS Parameter™ kit; R&D systems). Approximately 30 mg of each tissue was homogenized in a buffer consisting of 100 mM Tris-HCl, 2 mM EDTA, and 5 mM $MgCl_2 \cdot 6H_2O$ at pH 7.75 followed by centrifugation at 1600 *g* for 10 min at 4 °C. A part of the supernatant was reserved and stored at -80°C for the analysis of total scavenging oxidative capacity (TOSC; described below) and protein concentration (Bradford, 1976), while the remaining supernatant was used immediately for the determination of TBARS. For the analysis of TBARS, equal volumes of sample and acid reagent were combined and incubated for 15 min at room temperature. The sample was then centrifuged twice at 12000 *g* for 4 min at 4 °C and the supernatant was used for the assay. TBARS standards were prepared according to manufacturer instructions. The samples and standards were then incubated with TBA reagent (2:1 v/v) for 3 hrs at 50 °C, and absorbance was measured at 532 nm. TBARS levels were normalized to tissue protein concentration.

Total oxidative scavenging capacity (TOSC)

TOSC was determined as the rate of H_2O_2 removal, where H_2O_2 in the sample was monitored with Amplex Ultrared (Invitrogen). 100 µL of assay buffer (0.1 mM Amplex Ultrared, 1 U/mL horseradish peroxidase in 50 mM sodium citrate at pH 6.0) was added to 50 µL catalase standard (standards between 0 to 12 U of catalase activity were prepared) or sample (same homogenate prepared for the TBARS assay) in a spectrophotometer plate and pre-read at 565 nm. 50 µL of 160 µM H_2O_2 was then added to each well and the endpoint absorbance was measured after 5 min. The final TOSC was expressed as µmole H_2O_2/min (equivalent to 1 unit of catalase activity) and was normalized to tissue protein concentration.

Calculations and statistical analyses

Tissue GSH redox potential, MitoP/MitoB, TBARS and TOSC were measured in the four separate normoxic control samples taken during the exposures for both species (1 hr after MitoB injection, paired with the 6 hrs of hypoxia, 6 hrs of hyperoxia, and after an additional 1hr of recovery). As the normoxic values were not significantly different between these samples within a species (one-way ANOVA; data not shown), we grouped them into a single normoxia sample to compare with our O_2 treatment and recovery samples. For all measurements, hypoxic and hyperoxic groups had separate normoxic controls except for *S. marmoratus* GSH redox potential where the same normoxic control was used for hypoxic and hyperoxic groups due to low sample size.

Two-way ANOVA were performed to compare the effect of species (*O. maculosus* and *S. marmoratus*) and treatment (normoxia, 6 hrs hypoxia/hyperoxia treatment, and recovery from hypoxia/hyperoxia) on tissue GSH redox potential, MitoP/MitoB, TBARS, and TOSC. TBARS and TOSC were normalized to normoxic control values in order to investigate species-specific responses to hypoxia and hyperoxia exposure. Significant species by treatment interactions were followed with *posthoc* Holm-Sidak's multiple comparison to investigate within species treatment effects.

Results

Validation of MitoB use in marine sculpins

Within 30 min of injection into resting, normoxic *O. maculosus*, MitoB was detected in brain, gill and liver, after which there was an exponential loss of MitoB over 72 hrs post-injection (Fig.1A). MitoP, which is formed when MitoB is oxidized by mitochondrial H_2O_2, appeared quickly in the brain, gill, and liver, but at much lower concentrations than MitoB (Fig.1B). MitoP also showed an exponential loss over the 72 hrs post-injection (Fig.1B). In white muscle, MitoB and MitoP levels peaked at 1 hr after injection, but tissue concentrations were much lower compared with the other tissues sampled (highest levels at 1 hr with 0.167 MitoB and 0.06 MitoP pmol/mg tissue), so white muscle was not analysed for this study (see Supplementary Fig.3). Due to similar patterns of MitoP and MitoB loss from tissues, MitoP/MitoB was generally stable over 72 hr of consistent normoxic treatment (Fig.1C), but the higher levels of MitoP and Mito B detected over the first 8 hrs post-injection resulted in a high signal to noise ratio thus all experiments were completed within 8 hr of MitoB injection.

Brain

Hypoxia and hypoxia-recovery In both *O. maculosus* and *S. marmoratus* there were no significant effects of hypoxia or hypoxia followed by 1 hr of normoxic recovery (referred to as hypoxia-recovery from here on) on GSH redox potential or MitoP/MitoB ratio (Fig.2A&B; see Table 1 for ANOVA results). There was a significant effect of treatment and species on brain TBARS as well as a significant treatment by species interaction (Fig.2C; Table 1). Posthoc analysis revealed that *O. maculosus* had significantly higher TBARS during hypoxia exposure than in normoxia ($p=0.0012$) or when exposed to hypoxia-recovery ($p=0.017$), whereas in *S. marmoratus* there were no significant effects of hypoxia or hypoxia-recovery on brain TBARS. There were no significant effects of treatment or species on brain TOSC (Fig.2D; Table 1).

Hyperoxia and hyperoxia-recovery There was no effect of species, or hyperoxia and hyperoxia followed by 1 hr of normoxic recovery (referred to as hyperoxia-recovery from here on) treatment on GSH redox potential (Fig.2E; Table 2 for ANOVA results). There was a significant species effect on MitoP/MitoB, where *O. maculosus* had a higher MitoP/MitoB compared to *S. marmoratus* across treatments (Fig.2F; Table 2). There was a significant effect of species and a significant treatment by species interaction on TBARS (Fig.2G; Table 2). Post-hoc analysis revealed that *O. maculosus* had higher TBARS after hyperoxia exposure than in normoxia ($p=0.0013$), whereas there were no changes in TBARS in the brain of *S. marmoratus* in any treatment. There was a significant species effect on TOSC levels, where *O. maculosus* had higher TOSC levels than *S. marmoratus* (Fig.2H). There was no significant treatment effect on brain TOSC.

Liver

Hypoxia and hypoxia-recovery There was a significant effect of species, but no effect of treatment on liver GSH redox potential (Fig. 3A). The liver from *O. maculosus* had a more oxidized GSH redox potential than *S. marmoratus* (Fig.3A). There was also a significant species effect on MitoP/MitoB, where *O. maculosus* had higher MitoP/MitoB than *S. marmoratus* (Fig.3B). There was no effect of treatment on MitoP/MitoB. Neither species showed changes in liver TBARS and TOSC levels (Fig.3C&D; Table 1).

Hyperoxia and hyperoxia-recovery There were no effects of species or hyperoxia treatment on liver GSH redox potential (Fig.3E). There were significant species and treatment effects on MitoP/MitoB, where *O. maculosus* had higher MitoP/MitoB than *S. marmoratus* that increased during hyperoxia in both species (Fig.3F). There were no effects of species or treatment on liver TBARS (Fig.3G). There was a significant species effect and a treatment by species interaction on TOSC levels. Post-hoc analysis revealed that *S. marmoratus* had significantly higher TOSC levels in the hyperoxia treatment compared with normoxia ($p=0.0089$) and *O. maculosus* showed no changes with treatment (Fig.3H).

Gill

Hypoxia and hypoxia-recovery In the gills, there were no species or treatment effects on GSH redox potential (Fig.4A). There was a significant effect of treatment on MitoP/MitoB, where MitoP/MitoB was lower in the hypoxia and hypoxia-recovery treatments compared with the normoxic controls for both species (Fig.4B). There was a significant species effect on TBARS, where *S. marmoratus* generally showed higher TBARS than *O. maculosus*, especially in the hypoxia

and hypoxia-recovery treatments (Fig.4C). There were no changes to TOSC levels with treatment in either species (Fig.4D).

Hyperoxia and hyperoxia-recovery There was no species or treatment effect on gill GSH redox potential (Fig.4E; Table 2). There was a significant treatment effect on MitoP/MitoB, but no species effect. MitoP/MitoB progressively increased in both species following hyperoxia and hyperoxia-recovery exposure (Fig.4F). There were no changes to TBARS and TOSC levels in either species exposed to hyperoxia and hyperoxia-recovery (Fig.4G&H).

Discussion

The goal of the present study was to determine whether there were differences in *in vivo* ROS metabolism during exposure to hypoxia, hyperoxia and subsequent normoxic recovery between two species of sculpins that differ in hypoxia tolerance and inhabit environments that differ in the frequency and severity of O_2 fluctuations. We hypothesized that the more hypoxia tolerant species would be able to minimize the impacts of environmental O_2 variability on ROS metabolism such that oxidative stress would be lower than in the less hypoxia tolerant species. Our analysis demonstrated that the more hypoxia tolerant *O. maculosus* exhibited more oxidative damage in the brain following exposure to both hypoxia and hyperoxia (which recovered in normoxia) compared to the less tolerant *S. marmoratus*. In comparison, the responses in the liver and gills were relatively subtle compared with those in the brain of *O. maculosus,* and *S. marmoratus* showed more changes in response to O_2 fluctuations in these tissues. Overall, these data do not support our original hypothesis, which is likely due to the complex tissue and species-specific responses in ROS metabolism during environmental O_2 fluctuations. The relationship between ROS metabolism and hypoxia tolerance may also be further complicated by the role that ROS can play in cell signaling.

Our validation study demonstrated that MitoB uptake into isolated mitochondria from *O. maculosus* was similar to that observed in *Drosophila* (Supplementary Fig. 1; Cochemé et al., 2011). When MitoB was injected into *O. maculosus*, MitoB and MitoP were detected in brain, gill, and liver within 30 min of injections. The timeline of MitoB loss in marine sculpins, however, differed from that of the freshwater brown trout (Salin et al., 2015), possibly due to differences in osmoregulatory strategies. In brown trout, MitoB was still at high levels in liver at 72 hrs post-injection (94% of concentration at first measured timepoint of 3 hr; Salin et al. 2017), whereas the levels in the liver of *O. maculosus* were much lower at 72 hrs (0.5% of concentration at 0.5 hr; Fig.1). Despite the decreases in MitoB in tissues over time, the levels of MitoB present in the tissues of sculpins allowed us to reliably detect MitoB and MitoP for the required 8 hr duration

of our study. There were also differences in tissue MitoP/MitoB between sculpins and brown trout, with brown trout white muscle (0.27) showing a much higher ratio than in liver (0.073), whereas in the white muscle of sculpins there was a low uptake of MitoB, which rendered the calculation of MitoP/MitoB unreliable (Supplementary Fig. 3; Salin et al. 2017). Although we cannot explain the species-specific differences in white muscle MitoB uptake, the low uptake of MitoB in sculpin white muscle is consistent with its low mitochondrial content. It is also interesting to note that MitoB uptake was observed in the sculpin brain, which was not observed in mammals likely due to the presence of a tight blood brain barrier. Teleost fish are believed to also have a tight endothelial-based blood brain barrier analogous to that of other vertebrates, but the uptake of MitoB in sculpin brain suggests that there may be functional differences in the blood brain barrier between teleosts and mammals that allowed for MitoB uptake (Kniesel and Wolburg, 2000; Wolburg et al., 1983). These differences in MitoB uptake emphasize the importance of validating its use in different organisms and tissues, but overall, the results of our validation study suggest that MitoB can be used to reliably detect *in vivo* H_2O_2 accumulation in brain, liver and gill of sculpins over an 8 hr exposure window.

Net *in vivo* ROS accumulation is a product of ROS generation, which is affected by cellular redox environment, and ROS scavenging, which is also affected by redox environment and the antioxidants present (Aon et al., 2010). Tissue-specific differences in ROS-induced oxidative damage can be ascribed to variation in ROS generation capacity and susceptibility to oxidation (Murphy et al., 2011). In order to draw meaningful comparisons of ROS metabolism across tissues and between species, it is important to consider the drivers of ROS generation and the subsequent downstream effects of ROS accumulation in addition to measuring the amount of ROS generated. Therefore, in this comparative study, we chose to quantify representative measures of redox environment, mitochondrial ROS, ROS damage, and scavenging capacity. Although the indices we chose are not all encompassing (*e.g.* there are numerous cellular redox couples and we only measured one), they provide insight into the important components of ROS metabolism across tissues and reveal interspecific differences in whole animal responses to O_2 fluctuations.

In both species of sculpin and in all tissues examined, there were no O_2 treatment-associated changes in redox environment (as assessed by GSH redox potential), and no large changes in mitochondrial H_2O_2 in brain and liver. Our previous work in isolated mitochondria from these species demonstrated an association between experimentally manipulated GSH redox potential and H_2O_2 production, whereby additions of extramitochondrial GSH (to induce reductive stress)

resulted in increased in H_2O_2 production (Lau and Richards, 2019). We also demonstrated that mitochondria from these two species possessed similar capacities to buffer extramitochondrial reductive stress. In combination, these studies suggest that environmentally relevant changes in O_2 do not induce large changes in tissue GSH redox state in either species, which could explain why there are no large and consistent changes in H_2O_2 *in vivo*. It is important to point out however, that our sample size for the GSH redox analysis is low due to tissue sample limitations, so the precise relationship between *in vivo* GSH redox potential and H_2O_2 production should be viewed with caution. Furthermore, mitochondrial H_2O_2 emission did not differ between species except under oligomycin-induced state 4 respiration state (Lau and Richards, 2019), which represents a very specific set of conditions (*i.e.* where ATP synthase is completely inhibited) that do not occur *in vivo*. Thus, our observations at the whole animal level appears to be consistent with our previous *in vitro* study.

Despite the modest changes in mitochondrial H_2O_2 detected in all tissues using MitoB, we observed signs of oxidative stress in some tissues. For example, the large increases in TBARS in the brain of *O. maculosus* following hypoxia and hyperoxia exposure were not accompanied by significant changes in MitoP/MitoB during hypoxia exposure and recovery (Fig.2B), and the changes of MitoP/MitoB during hyperoxia and recovery were subtle and only differentiated by species (Fig.2F). There are several possible explanations for this discrepancy. First, the oxidative damage observed in the brain of *O. maculosus* could have been caused by ROS released by ETS complex sites oriented toward the cytoplasmic side (*i.e.* complex III and glycerol-3-phosphate dehydrogenase; Quinlan et al., 2013) and not detected by MitoB, which is localized to the mitochondrial matrix. Second, ROS other than H_2O_2 (*e.g.* superoxide and hydroxyl radicals which are normally quickly scavenged and converted to less reactive H_2O_2), and reactive species other than ROS (*e.g.* reactive sulfur and nitrogen species; DeLeon et al., 2016) may be causing oxidative damage in response to O_2 stress. Third, non-mitochondrial sites of ROS production, *e.g.* microsomes and peroxisomes, may be responsible for the observed oxidative damage (Brown and Borutaite, 2012; Chance et al., 1979). Despite these caveats that come with using MitoB to detect mitochondrial H_2O_2, the lack of a direct connection between ROS generation and presumed downstream effects of ROS is not unique to this study and has been observed in other organisms. For example, in molluscs exposed to anoxia- and hypoxia-recovery, changes in aconitase activity (the inhibition of which is directly related to the presence of superoxide) did not mirror changes in total antioxidant capacity nor measures of oxidative damage (Ivanina and Sokolova 2016). These results illustrate the importance of taking a multifaceted approach to

understanding ROS metabolism since measuring only one aspect *e.g.* oxidative damage, may potentially be misleading.

While we predicted that the more O_2 sensitive brain would show less oxidative damage compared to liver and gills, especially in the hypoxia tolerant *O. maculosus*, in fact, we observed the opposite where the brain of *O. maculosus* accumulated high levels of TBARS during hypoxia and hyperoxia exposure. In contrast, the same O_2 stressors did not result in any measurable TBARS in the brain of *S. marmoratus*. Tissue specificity in oxidative damage has been observed in other studies (Johansson et al. 2018; Lushchak et al. 2005; Lushchak and Bagnyukova 2007), with no consistent pattern of tissues being similarly impacted with changes to environmental O_2. In addition, there were no consistent patterns among the types of oxidative damage detected, *e.g.* protein carbonyls, lipid peroxides, and TBARS, within a tissue during the hypoxia-recovery exposures in these studies. Species and tissue differences in the extent and type of oxidative damage observed could be related to inherent variation in their susceptibility to oxidative damage, *e.g.* due to differences in membrane lipid composition (Tribble et al., 1992) or level of misfolded proteins (Dukan et al., 2000). Our assessment of oxidative damage was limited to TBARS and it is possible that other markers of lipid peroxidation (*e.g.* 4-hydroxynonenal and lipid peroxides) or markers of other types of oxidative damage (*e.g.* protein carbonyls, mtDNA damage) would offer additional insights into the downstream effects of ROS. Differences in antioxidant mechanisms could also contribute to explaining species and tissue variation in the levels of oxidative damage measured (Leveelahti et al., 2014; Welker et al., 2012). In the present study, only the liver of *S. marmoratus* experienced changes in TOSC in response to hyperoxia. The lack of change in TOSC in the other tissues in both species could indicate that the existing levels of antioxidants were sufficient to minimize H_2O_2 accumulation and oxidative damage, and/or that other antioxidants mechanisms targeting non-H_2O_2 reactive species were involved since our assessment of TOSC only captures H_2O_2 metabolism.

Interpreting the species-specific effects of changes in environmental O_2 on ROS metabolism is further complicated by the fact that ROS and the products of oxidative damage can play important roles in cell signaling (Ayala et al., 2014; Sies, 2017; Wong et al., 2008). For example, malondialdehyde (the lipid peroxidation product quantified by the TBARS assay) and other lipid peroxidation adducts can act as secondary messengers of free radicals that subsequently affect protein function and structure, after which they can be enzymatically metabolized (Ayala et al. 2015; Zarkovic et al. 2013). As a result, the increases in TBARS observed in the brain of *O. maculosus* during hypoxia and hyperoxia exposure, could be part of a signaling process to

coordinate physiological responses to changes in environmental O_2 levels. In organisms that inhabit the environmentally dynamic higher intertidal, such as *O. maculosus*, these putative signaling mechanisms may be important and possibly confer a survival advantage. Consistent with the idea that TBARS may serve as a signaling molecule in the brain of *O. maculosus* is the fact that TBARS levels quickly recovered to control values after 1 hr of normoxic recovery from hypoxia, possibly due to this tissue possessing a higher capacity to repair lipid peroxidation. Also, *O. maculosus* displayed this transient response despite being exposed to a relatively less severe level of hypoxia as compared to *S. marmoratus.* Further studies are necessary to directly test whether lipid peroxidation products and other products of oxidative damage play an important role in cell signaling during exposure to environmental O_2 variability.

One of the main challenges associated with interpreting tissue responses to whole-animal hypoxia or hyperoxia exposure across species is taking into account their species-specific physiological modifications to the O_2 transport cascade. For example, when species are exposed to the same level of environmental hypoxia and hyperoxia, physiological adjustments to the O_2 transport cascade may not yield similar tissue PO_2. Indeed, it must be noted here that our choice of hypoxic PO_2 used herein represents a more severe hypoxic stress for *S. marmoratus* than *O. maculosus*, but it is interesting that the observed responses are generally greater in *O. maculosus* than *S. marmoratus*, perhaps due to a hypoxia-induced inhibition of metabolism in the latter species. Attempts to scale hypoxia exposures to species-specific indices of hypoxia tolerance (*e.g.* P_{crit}) do not appear to fully normalize tissue O_2 exposures or physiological responses (Mandic et al., 2014; Speers-Roesch et al., 2012). The impact of these species-specific physiological adjustments on tissue PO_2 should, however, be minimized at the respiratory surface that interacts directly with the environment. Indeed, in both species examined here, gill mitochondrial H_2O_2 production during hypoxia and hyperoxia exposures were similar, suggesting similar levels of O_2 stress. During hypoxia exposure, the decrease in ROS production observed in both species is likely due to the lower availably of O_2 substrate for ROS production (Fig.4B), however, recovery from hypoxic stress is generally thought to lead to an increase of H_2O_2 generation. This was not observed in the sculpin gills and in fact both species decreased mitochondrial H_2O_2 in response to hypoxia-recovery (Fig.4B). The lower H_2O_2 after hypoxia-recovery could be due to an active suppression of mitochondrial H_2O_2 generation in both species exposed to a similar hypoxic PO_2 at the gills. In *S. marmoratus*, however, this decrease in mitochondrial H_2O_2 appears to be concomitant with higher TBARS levels (although only a significant species effect, with treatment effect approaching significance, $p=0.071$; Table 1) during both hypoxia and hypoxia-recovery compared to *O. maculosus*, suggesting that *S. marmoratus* still experienced oxidative

damage. Hyperoxia and hyperoxia-recovery yielded the expected increases in mitochondrial H_2O_2 in both species, as O_2 is abundant and it further increases in normoxic recovery suggesting that ROS production can be sensitive to O_2 fluctuations even at supraphysiological O_2 tensions (Fig.4F).

Summary

Overall, we observed that the more hypoxia tolerant sculpin *O. maculosus* differed in tissue responses to O_2 variability when compared to the less hypoxia tolerant *S. marmoratus*. We observed *in vivo* responses in the brain that suggests that hypoxia tolerance may not necessarily be related to an overall decrease in ROS generation to minimize oxidative stress, but these responses were also dependent on the tissue and the PO_2 in question. While lowering ROS emission and minimizing oxidative damage has been suggested as a putatively adaptive response to O_2 limitation in other hypoxia tolerant animals (assessed in gastrocnemius muscle in high-altitude deer mice, *Peromyscus maniculatus* and liver in killifish; Du et al., 2016; Mahalingam et al., 2017), our *in vivo* and *in vitro* observations (Lau and Richards 2019) of the hypoxia tolerant *O. maculosus* suggests that minimizing ROS and oxidative damage may not be a universal adaptive strategy to inhabiting O_2 variable environments. The species and tissue specificity observed in this study and others is likely due to the multi-dimensional nature of environmental O_2 variation that animals experience in diverse habitats (Mandic and Regan, 2018), and potentially complicated by the fact that ROS can also act as a signaling molecule (Dickinson and Chang 2011).

Acknowledgements

We would like to thank Joshua Emerman, Monica Goldade, Dr. Tammy Rodela, Derek Somo, and Andrew Thompson for their help with fish collections, and to Dr. Rodela and D. Somo for helping with tissue sampling.

Competing Interests

The authors declare no competing or financial interests.

Funding

This work was funded by a Natural Sciences and Engineering Research Council of Canada (NSERC) Discovery grant to J.G.R, and by a Wellcome Trust Investigator Award (110159/Z/15/Z) to M.P.M. G.Y.L. was supported by a NSERC Canada Graduate Scholarship, Michael Smith Foreign Supplement, and Company of Biologists Travel Grant.

Bibliography

Aon, M. A., Cortassa, S. and O'Rourke, B. (2010). Redox-optimized ROS balance: A unifying hypothesis. Biochim. Biophys. Acta BBA - Bioenerg. 1797, 865–877.

Ayala, A., Muñoz, M. F. and Argüelles, S. (2014). Lipid peroxidation: Production, metabolism, and signaling mechanisms of malondialdehyde and 4-hydroxy-2-nonenal. Oxid. Med. Cell. Longev. 2014, 1–31.

Bradford, M. M. (1976). A rapid and sensitive method for the quantitation of microgram quantities of protein utilizing the principle of protein-dye binding. Anal. Biochem. 72, 248–254.

Brand, M. D. (2000). Uncoupling to survive? The role of mitochondrial inefficiency in ageing. Exp. Gerontol. 35, 811–820.

Brown, G. C. and Borutaite, V. (2012). There is no evidence that mitochondria are the main source of reactive oxygen species in mammalian cells. Mitochondrion 12, 1–4.

Cadet, J. (2003). Oxidative damage to DNA: formation, measurement and biochemical features. Mutat. Res. Mol. Mech. Mutagen. 531, 5–23.

Chance, B., Sies, H. and Boveris, A. (1979). Hydroperoxide metabolism in mammalian organs. Physiol. Rev. 59, 527–605.

Chouchani, E. T., Pell, V. R., Gaude, E., Aksentijević, D., Sundier, S. Y., Robb, E. L., Logan, A., Nadtochiy, S. M., Ord, E. N. J., Smith, A. C., et al. (2014). Ischaemic accumulation of succinate controls reperfusion injury through mitochondrial ROS. Nature 515, 431–435.

Cochemé, H. M., Quin, C., McQuaker, S. J., Cabreiro, F., Logan, A., Prime, T. A., Abakumova, I., Patel, J. V., Fearnley, I. M., James, A. M., et al. (2011). Measurement of H_2O_2 within living drosophila during aging using a ratiometric mass spectrometry probe targeted to the mitochondrial matrix. Cell Metab. 13, 340–350.

Cochemé, H. M., Logan, A., Prime, T. A., Abakumova, I., Quin, C., McQuaker, S. J., Patel, J., Fearnley, I., James, A., Porteous, C., et al. (2012). Using the mitochondria-targeted ratiometric mass spectrometry probe MitoB to measure H_2O_2 in living Drosophila. Nat. Protoc. 7, 946–958.

D'Autréaux, B. and Toledano, M. B. (2007). ROS as signalling molecules: mechanisms that generate specificity in ROS homeostasis. Nat. Rev. Mol. Cell Biol. 8, 813–824.

DeLeon, E. R., Gao, Y., Huang, E., Arif, M., Arora, N., Divietro, A., Patel, S. and Olson, K. R. (2016). A case of mistaken identity: are reactive oxygen species actually reactive sulfide species? Am. J. Physiol. Regul. Integr. Comp. Physiol. 310, R549-560.

Du, S. N. N., Mahalingam, S., Borowiec, B. G. and Scott, G. R. (2016). Mitochondrial physiology and reactive oxygen species production are altered by hypoxia acclimation in killifish (*Fundulus heteroclitus*). J. Exp. Biol. 219, 1130–1138.

Dukan, S., Farewell, A., Ballesteros, M., Taddei, F., Radman, M. and Nystrom, T. (2000). Protein oxidation in response to increased transcriptional or translational errors. Proc. Natl. Acad. Sci. 97, 5746–5749.

Gutteridge, J. M. (1995). Lipid peroxidation and antioxidants as biomarkers of tissue damage. Clin. Chem. 41, 1819–1829.

Hickey, A. J. R., Renshaw, G. M. C., Speers-Roesch, B., Richards, J. G., Wang, Y., Farrell, A. P. and Brauner, C. J. (2012). A radical approach to beating hypoxia: depressed free radical release from heart fibres of the hypoxia-tolerant epaulette shark (Hemiscyllum ocellatum). J. Comp. Physiol. B 182, 91–100.

Ivanina, A. V. and Sokolova, I. M. (2016). Effects of intermittent hypoxia on oxidative stress and protein degradation in molluscan mitochondria. J. Exp. Biol. 219, 3794–3802.

Kniesel, U. and Wolburg, H. (2000). Tight junctions of the blood – brain barrier. Cell. Mol. Neurobiol. 20, 57–76.

Lau, G. Y. and Richards, J. G. (2018). Interspecific variation in brain mitochondrial complex I and II capacity and ROS emission in marine sculpins. J. Exp. Biol. jeb.189407.

Lau, G. Y., Mandic, M. and Richards, J. G. (2017). Evolution of Cytochrome *c* oxidase in hypoxia tolerant sculpins (Cottidae, Actinopterygii). Mol. Biol. Evol. 34, 2153–2162.

Leveelahti, L., Rytkönen, K. T., Renshaw, G. M. C. and Nikinmaa, M. (2014). Revisiting redox-active antioxidant defenses in response to hypoxic challenge in both hypoxia-tolerant and hypoxia-sensitive fish species. Fish Physiol. Biochem. 40, 183–191.

Logan, A., Cochemé, H. M., Li Pun, P. B., Apostolova, N., Smith, R. A. J., Larsen, L., Larsen, D. S., James, A. M., Fearnley, I. M., Rogatti, S., et al. (2014). Using exomarkers to assess mitochondrial reactive species *in vivo*. Biochim. Biophys. Acta BBA- General Subjects 1840: 923–930.

Mahalingam, S., McClelland, G. B. and Scott, G. R. (2017). Evolved changes in the intracellular distribution and physiology of muscle mitochondria in high-altitude native deer mice. J. Physiol. 595, 4785–4801.

Mandic, M. and Regan, M. D. (2018). Can variation among hypoxic environments explain why different fish species use different hypoxic survival strategies? J. Exp. Biol. 221, jeb161349.

Mandic, M., Sloman, K. A. and Richards, J. G. (2009a). Escaping to the surface: a phylogenetically independent analysis of hypoxia-induced respiratory behaviors in sculpins. Physiol. Biochem. Zool. 82, 730–738.

Mandic, M., Todgham, A. E. and Richards, J. G. (2009b). Mechanisms and evolution of hypoxia tolerance in fish. Proc. R. Soc. B Biol. Sci. 276, 735–744.

Mandic, M., Ramon, M. L., Gracey, A. Y. and Richards, J. G. (2014). Divergent transcriptional patterns are related to differences in hypoxia tolerance between the intertidal and the subtidal sculpins. Mol. Ecol. 23, 6091–6103.

Munro, D. and Treberg, J. R. (2017). A radical shift in perspective: mitochondria as regulators of reactive oxygen species. J. Exp. Biol. 220, 1170–1180.

Murphy, M. P., Holmgren, A., Larsson, N.-G., Halliwell, B., Chang, C. J., Kalyanaraman, B., Rhee, S. G., Thornalley, P. J., Partridge, L., Gems, D., et al. (2011). Unraveling the biological roles of reactive oxygen species. Cell Metab. 13, 361–366.

Niknahad, H., Khan, S. and O'Brien, P. J. (1995). Hepatocyte injury resulting from the inhibition of mitochondrial respiration at low oxygen concentrations involves reductive stress and oxygen activation. Chem. Biol. Interact. 98, 27–44.

Quinlan, C. L., Perevoschikova, I. V., Goncalves, R. L. S., Hey-Mogensen, M. and Brand, M. D. (2013). The determination and analysis of site-specific rates of mitochondrial reactive oxygen species production. Methods Enzymol. 526, 189-217.

Rahman, I., Kode, A. and Biswas, S. (2006). Assay for quantitative determination of glutathione and glutathione disulfide levels using enzymatic recycling method. Nat. Protoc. 1, 3159–3165.

Reznick, A. Z. and Packer, L. (1994). Oxidative damage to proteins: Spectrophotometric method for carbonyl assay. Methods Enzymol. 233, 357–363.

Richards, J. G. (2011). Physiological, behavioral and biochemical adaptations of intertidal fishes to hypoxia. J. Exp. Biol. 214, 191–199.

Salin, K., Auer, S. K., Rudolf, A. M., Anderson, G. J., Cairns, A. G., Mullen, W., Hartley, R. C., Selman, C. and Metcalfe, N. B. (2015). Individuals with higher metabolic rates have lower levels of reactive oxygen species *in vivo*. Biol. Lett. 11, 20150538.

Salin, K., Auer, S. K., Villasevil, E. M., Anderson, G. J., Cairns, A. G., Mullen, W., Hartley, R. C. and Metcalfe, N. B. (2017). Using the MitoB method to assess levels of reactive oxygen species in ecological studies of oxidative stress. Sci. Rep. 7, 41228.

Schafer, F. Q. and Buettner, G. R. (2001). Redox environment of the cell as viewed through the redox state of the glutathione disulfide/glutathione couple. Free Radic. Biol. Med. 30, 1191–1212.

Scott, G. R., Egginton, S., Richards, J. G. and Milsom, W. K. (2009). Evolution of muscle phenotype for extreme high altitude flight in the bar-headed goose. Proc. R. Soc. B Biol. Sci. 276, 3645–3653.

Sies, H. (2017). Hydrogen peroxide as a central redox signaling molecule in physiological oxidative stress: Oxidative eustress. Redox Biol. 11, 613–619.

Speers-Roesch, B., Richards, J. G., Brauner, C. J., Farrell, A. P., Hickey, A. J. R., Wang, Y. S. and Renshaw, G. M. C. (2012). Hypoxia tolerance in elasmobranchs. I. Critical oxygen tension as a measure of blood oxygen transport during hypoxia exposure. J. Exp. Biol. 215, 93–102.

Storz, J. F., Runck, A. M., Sabatino, S. J., Kelly, J. K., Ferrand, N., Moriyama, H., Weber, R. E. and Fago, A. (2009). Evolutionary and functional insights into the mechanism underlying high-altitude adaptation of deer mouse hemoglobin. Proc. Natl. Acad. Sci. 106, 14450–14455.

Tribble, D. L., Holl, L. G., Wood, P. D. and Krauss, R. M. (1992). Variations in oxidative susceptibility among six low density lipoprotein subfractions of differing density and particle size. Atherosclerosis 93, 189–199.

Welker, A. F., Campos, É. G., Cardoso, L. A. and Hermes-Lima, M. (2012). Role of catalase on the hypoxia/reoxygenation stress in the hypoxia-tolerant Nile tilapia. Am. J. Physiol.-Regul. Integr. Comp. Physiol. 302, R1111–1118.

Wolburg, H., Kastner, R. and Kurz-Isler, G. (1983). Lack of orthogonal particle assemblies and presence of tight junctions in astrocytes of the goldfish (*Carassius auratus*). A freeze-fracture study. Cell Tissue Res. 234, 389–402.

Wong, C. M., Cheema, A. K., Zhang, L. and Suzuki, Y. J. (2008). Protein carbonylation as a novel mechanism in redox signaling. Circ. Res. 102, 310–318.

Yusa, T., Beckman, J. S., Crapo, J. D. and Freeman, B. A. (1987). Hyperoxia increases H_2O_2 production by brain *in vivo*. J. Appl. Physiol. 63, 353–358.

Figures

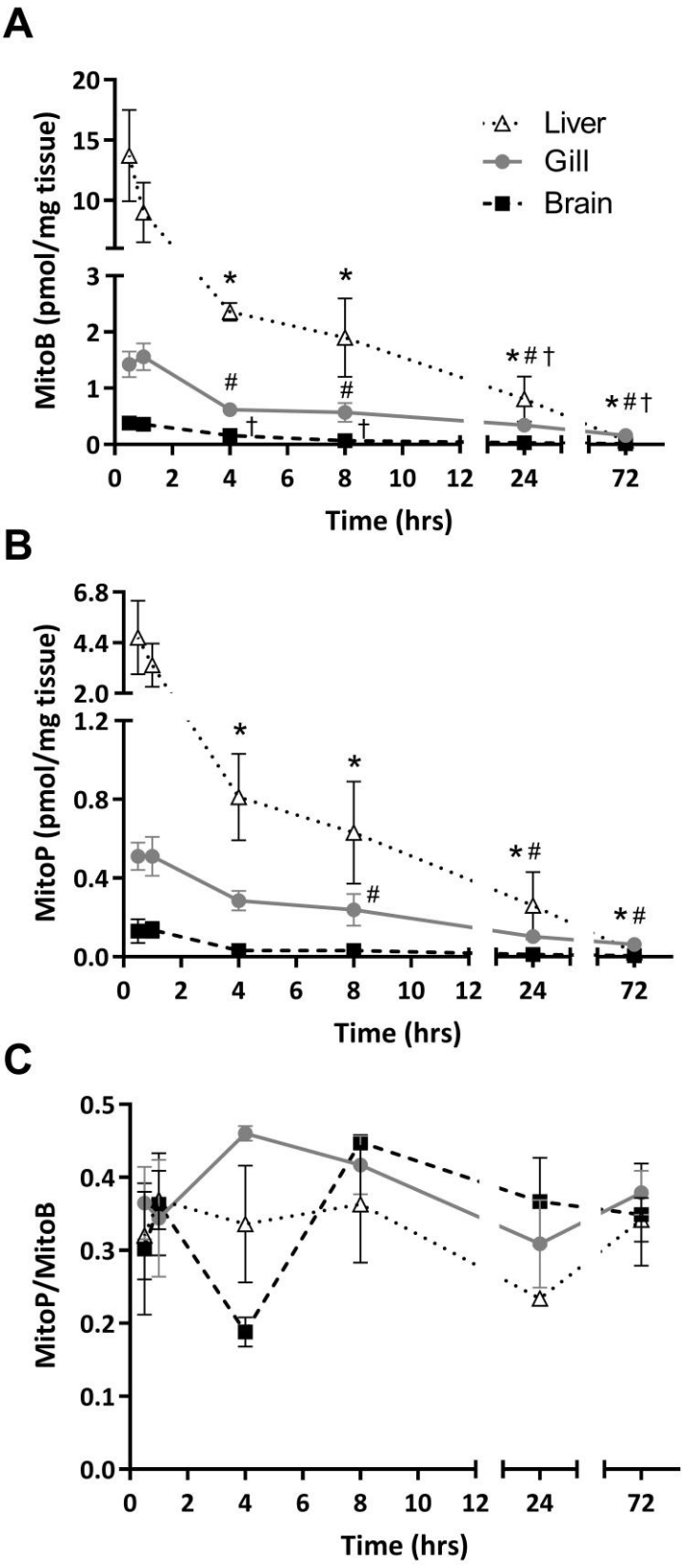

Figure 1. (A) MitoB, (B) MitoP, and (C) MitoP/MitoB in liver (hollow black triangle), gill (grey circle), and brain (solid black square) over 72hrs post-injection of MitoB in normoxic, resting *O. maculosus* (n=3). One-way ANOVA with Tukey's multiple comparisons test was used to assess the effects of time in each tissue. The symbols (* for liver, # for gills, † for brain) indicate significant differences ($P<0.05$) from the 0.5 hr timepoint. There were no significant effects of time on MitoP/MitoB in any tissues ($p= 0.39$, 0.14, and 0.59 for liver, gills and brain respectively). See supplementary materials for data on white muscle.

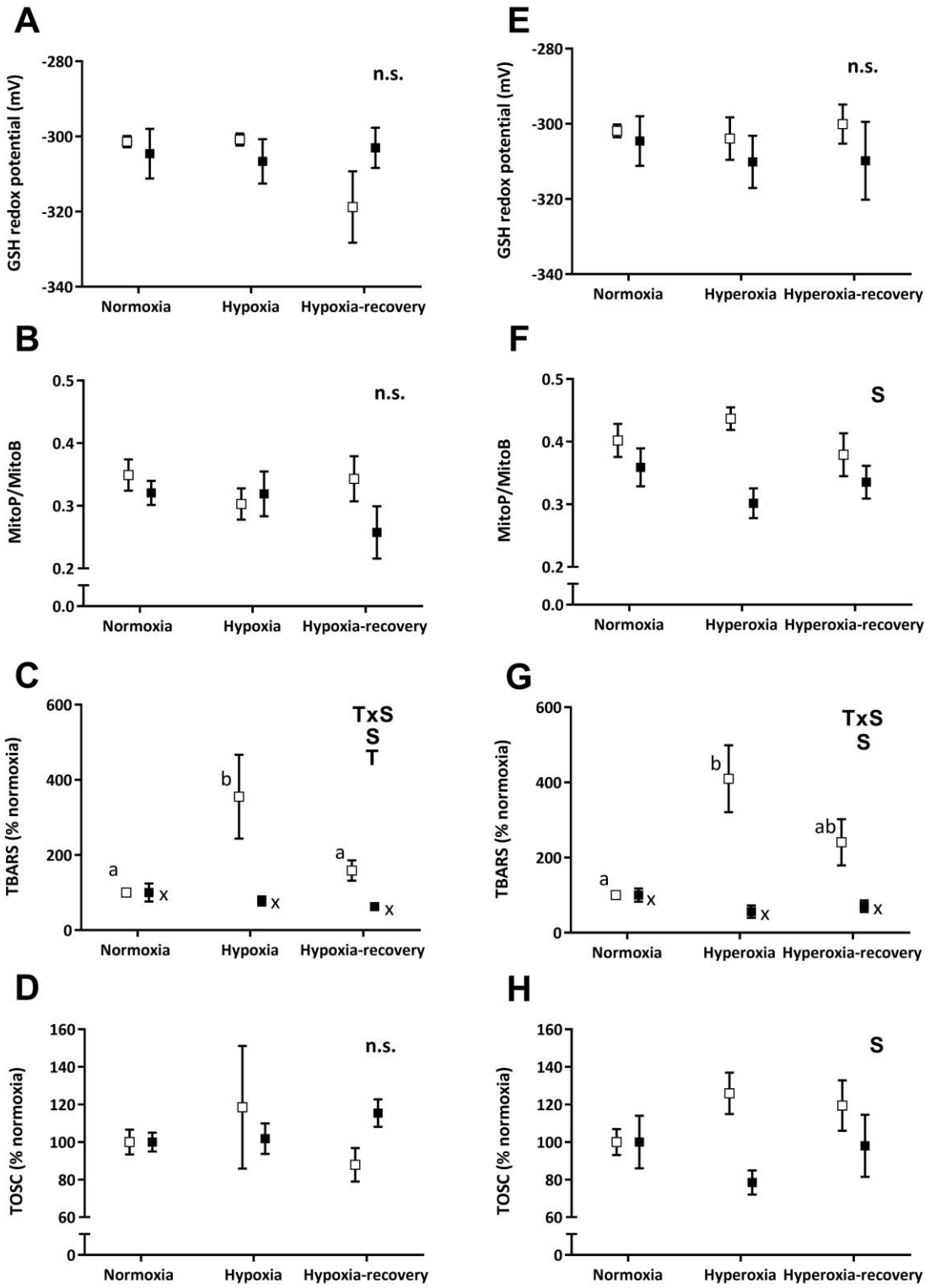

Figure 2. The effect of hypoxia (3.5kPa)-recovery (A-D) and hyperoxia (64.0kPa)-recovery (E-H) in brain of *Oligocottus maculosus* (hollow squares) and *Scorpaenichthys marmoratus* (solid squares) on ROS metabolism as assessed by (A, E) tissue GSH redox potential, (B, F) MitoP/MitoB, (C, G) TBARS (normalized to normoxia control value), (D, H) TOSC (normalized to normoxia control value). Data are means ± standard error of mean. "**T**" indicates significant treatment effect, "**S**" indicates significant species effect, "**TxS**" indicates significant treatment by species interaction, and "n.s." denotes no statistical significance. Letters indicate results from posthoc Sidak's multiple comparison within species treatment effect.

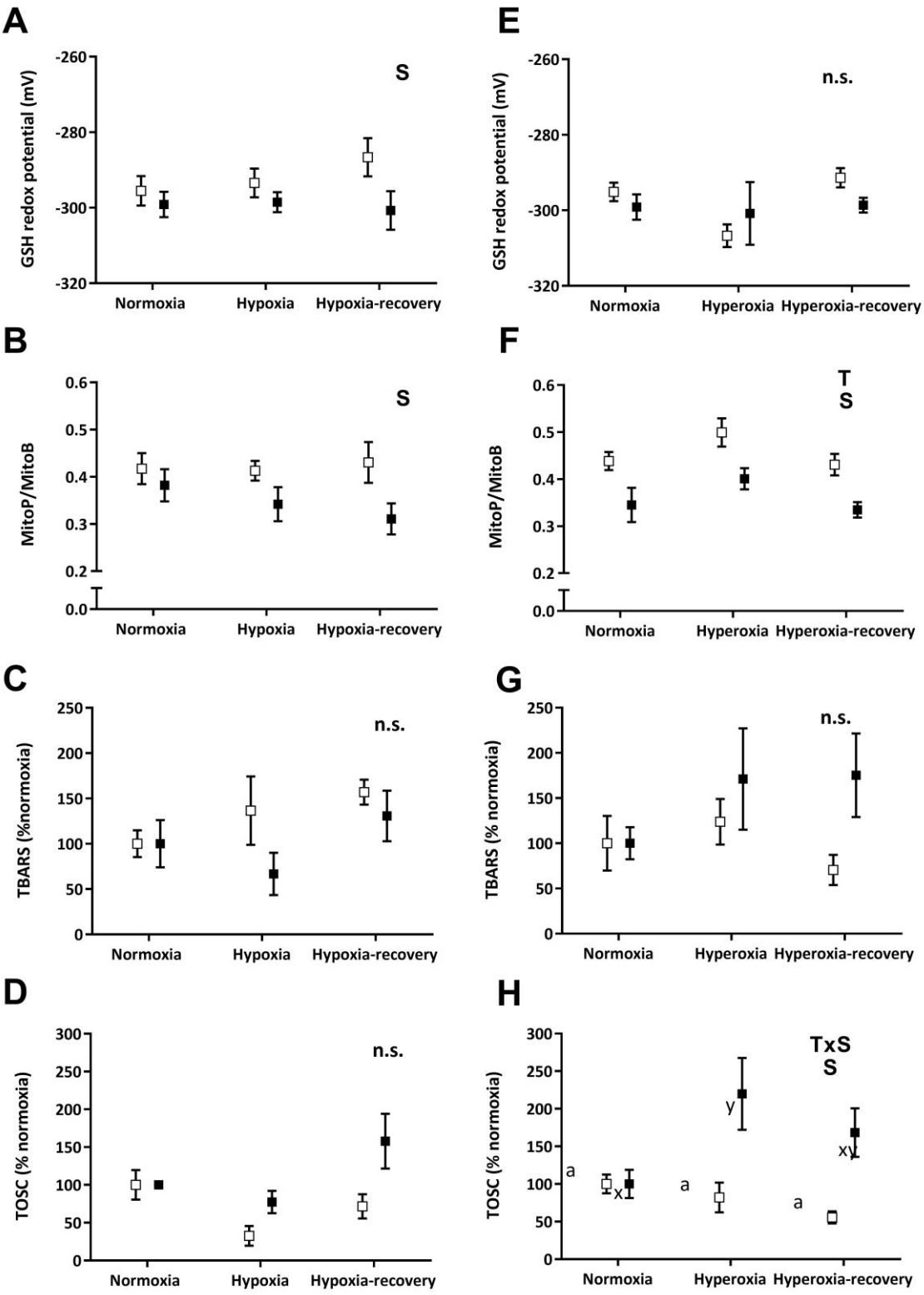

Figure 3. The effect of hypoxia (3.5kPa)-recovery (A-D) and hyperoxia (64.0kPa)-recovery (E-H) in liver of *Oligocottus maculosus* (hollow squares) and *Scorpaenichthys marmoratus* (solid squares) on ROS metabolism as assessed by (A, E) tissue GSH redox potential, (B, F) MitoP/MitoB, (C, G) TBARS (normalized to normoxia control value), (D, H) TOSC (normalized to normoxia control value). Data are means ± standard error of mean. "**T**" indicates significant treatment effect, "**S**" indicates significant species effect, "**TxS**" indicates significant treatment by species interaction, and "n.s." denotes no statistical significance. Letters indicate results from posthoc Sidak's multiple comparison within species treatment effect.

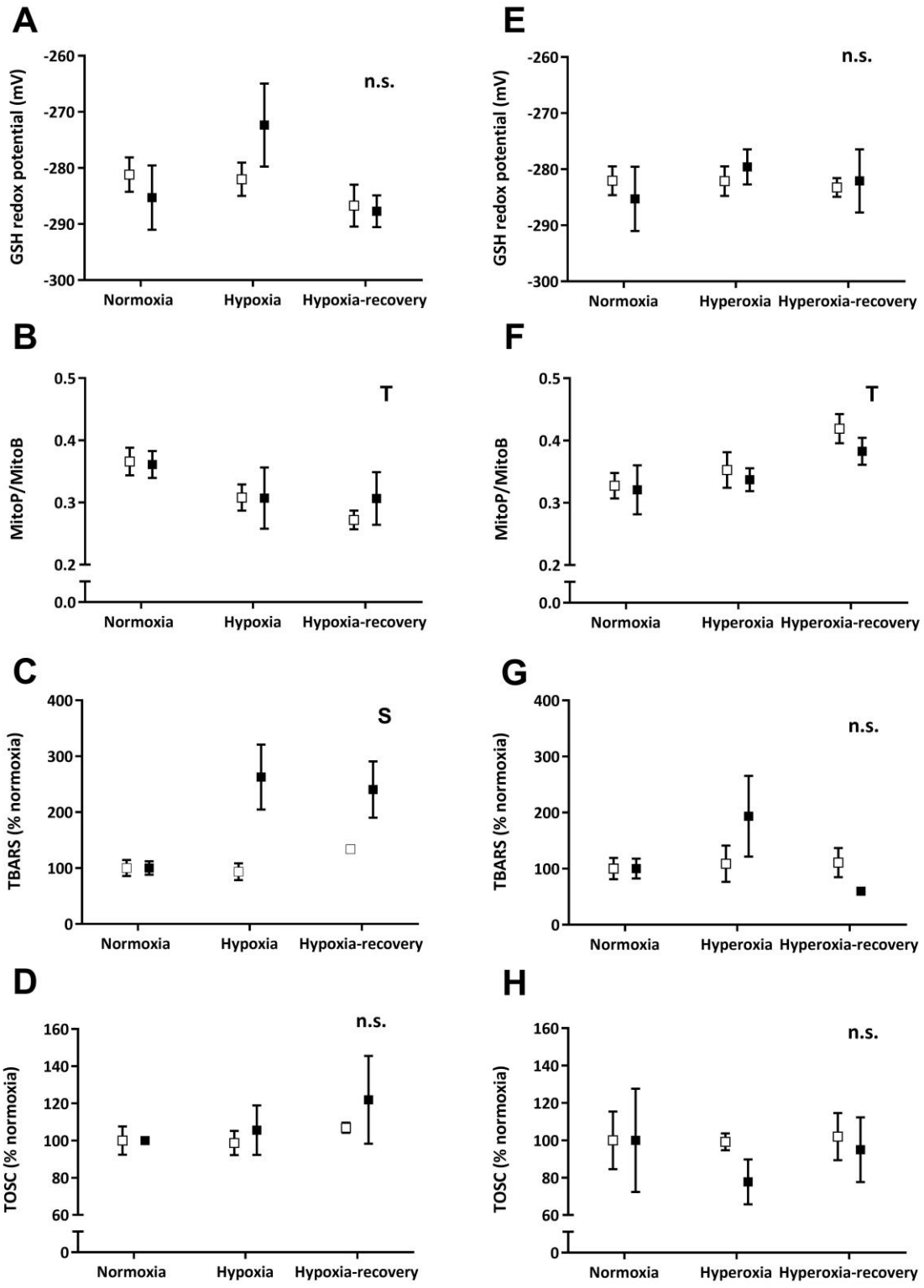

Figure 4. The effect of hypoxia (3.5kPa)-recovery (A-D) and hyperoxia (64.0kPa)-recovery (E-H) in gill of *Oligocottus maculosus* (hollow squares) and *Scorpaenichthys marmoratus* (solid squares) on ROS metabolism as assessed by (A, E) tissue GSH redox potential, (B, F) MitoP/MitoB, (C, G) TBARS (normalized to normoxia control value), (D, H) TOSC (normalized to normoxia control value). Data are means ± standard error of mean. "**T**" indicates significant treatment effect, "**S**" indicates significant species effect, "**TxS**" indicates significant treatment by species interaction, and "n.s." denotes no statistical significance. Letters indicate results from posthoc Sidak's multiple comparison within species treatment effect.

Table 1. Two-way ANOVA results for 3.5 kPa hypoxia and hypoxia-recovery exposure for both species. For sample size, the numbers from left to right correspond to the data points shown in the appropriate panel from Fig. 2, 3, and 4 (O= *O. maculosus* and S= *S. marmoratus*).

Tissue	Variable	Main Effect Variable	F	P value	Significance	Sample size
Brain	GSH redox potential	Treatment	1.03	0.37	ns	O (n=5, 3, 3); S (n=5, 3, 7)
		Species	0.21	0.65	ns	
		Treatment x Species	1.86	0.18	ns	
Brain	MitoP/MitoB	Treatment	0.64	0.53	ns	O (n=9, 6, 6); S (n=6, 6, 6)
		Species	1.64	0.21	ns	
		Treatment x Species	1.33	0.28	ns	
Brain	TBARS	**Treatment**	**4.52**	**0.023**	*	O (n=5, 4, 4); S (n=4, 5, 5)
		Species	**12.67**	**0.002**	**	
		Treatment x Species	**5.41**	**0.013**	*	
Brain	TOSC	Treatment	0.30	0.74	ns	O (n=4, 4, 4); S (n=4, 5, 5)
		Species	0.098	0.76	ns	
		Treatment x Species	1.27	0.31	ns	
Liver	GSH redox potential	Treatment	0.35	0.71	ns	O (n=7, 4, 4); S (n=5, 3, 3)
		Species	**4.44**	**0.048**	*	
		Treatment x Species	0.82	0.45	ns	
Liver	MitoP/MitoB	Treatment	0.37	0.70	ns	O (n=10, 6, 7); S (n=6, 7, 6)
		Species	**6.68**	**0.014**	*	
		Treatment x Species	0.71	0.50	ns	
Liver	TBARS	Treatment	1.62	0.22	ns	O (n=6, 6, 5); S (n=4, 5, 8)
		Species	2.02	0.17	ns	
		Treatment x Species	0.82	0.45	ns	
Liver	TOSC	Treatment	2.79	0.079	ns	O (n=6, 5, 5); S (n=4, 5, 8)
		Species	4.11	0.053	ns	
		Treatment x Species	1.34	0.28	ns	
Gill	GSH redox potential	Treatment	2.39	0.12	ns	O (n=6, 4, 4); S (n=5, 4, 4)
		Species	0.16	0.69	ns	
		Treatment x Species	1.21	0.32	ns	
Gill	MitoP/MitoB	**Treatment**	**13.41**	**0.045**	*	O (n=9, 7, 7); S (n=6, 6, 6)
		Species	0.16	0.70	ns	
		Treatment x Species	0.27	0.77	ns	
Gill	TBARS	Treatment	2.90	0.071	ns	O (n=6, 6, 6); S (n=4, 8, 5)
		Species	**8.02**	**0.0083**	**	
		Treatment x Species	2.32	0.12	ns	
Gill	TOSC	Treatment	0.82	0.45	ns	O (n=7, 6, 6); S (n=4, 8, 5)
		Species	0.54	0.47	ns	
		Treatment x Species	0.19	0.83	ns	

Table 2. Two-way ANOVA results for 64 kPa hyperoxia and hyperoxia-recovery exposure. For sample size, the numbers from left to right correspond to the data points shown in the appropriate panel from Fig. 2, 3, and 4 (O= *O. maculosus* and S= *S. marmoratus*).

Tissue	Variable	Main Effect Variable	F	P value	Significance	Sample size
Brain	GSH redox potential	Treatment	0.16	0.85	ns	O (n=4, 3, 3); S (n=5, 3, 3)
		Species	1.33	0.27	ns	
		Treatment x Species	0.14	0.87	ns	
Brain	MitoP/MitoB	Treatment	0.35	0.71	ns	O (n=9, 6, 4); S (n=6, 6, 6)
		Species	**10.58**	**0.0028**	**	
		Treatment x Species	1.80	0.18	ns	
Brain	TBARS	Treatment	3.43	0.053	ns	O (n=4, 4, 6); S (n=4, 4, 4)
		Species	**17.53**	**0.0005**	***	
		Treatment x Species	**6.01**	**0.009**	**	
Brain	TOSC	Treatment	0.27	0.77	ns	O (n=5, 4, 6); S (n=4, 4, 4)
		Species	**5.22**	**0.033**	*	
		Treatment x Species	1.87	0.18	ns	
Liver	GSH redox potential	Treatment	2.89	0.08	ns	O (n=7, 3, 3); S (n=5, 3, 4)
		Species	0.33	0.57	ns	
		Treatment x Species	1.62	0.22	ns	
Liver	MitoP/MitoB	**Treatment**	**4.24**	**0.023**	*	O (n=9, 6, 7); S (n=6, 6, 6)
		Species	**21.96**	**<0.0001**	****	
		Treatment x Species	0.0055	0.99	ns	
Liver	TBARS	Treatment	1.00	0.37	ns	O (n=9, 6, 7); S (n=6, 6, 6)
		Species	3.41	0.078	ns	
		Treatment x Species	1.22	0.31	ns	
Liver	TOSC	Treatment	2.45	0.11	ns	O (n=6, 5, 5); S (n=4, 4, 4)
		Species	**18.02**	**0.0003**	***	
		Treatment x Species	**4.64**	**0.021**	*	
Gill	GSH redox potential	Treatment	0.28	0.76	ns	O (n=7, 4, 5); S (n=5, 4, 4)
		Species	0.0029	0.96	ns	
		Treatment x Species	0.32	0.73	ns	
Gill	MitoP/MitoB	**Treatment**	**4.67**	**0.016**	*	O (n=7, 4, 5); S (n=5, 5, 4)
		Species	0.85	0.36	ns	
		Treatment x Species	0.17	0.84	ns	
Gill	TBARS	Treatment	1.58	0.23	ns	O (n=6, 5, 3); S (n=5, 5, 4)
		Species	0.12	0.73	ns	
		Treatment x Species	1.55	0.23	ns	
Gill	TOSC	Treatment	0.28	0.76	ns	O (n=7, 6, 4); S (n=5, 5, 4)
		Species	0.49	0.49	ns	
		Treatment x Species	0.21	0.81	ns	

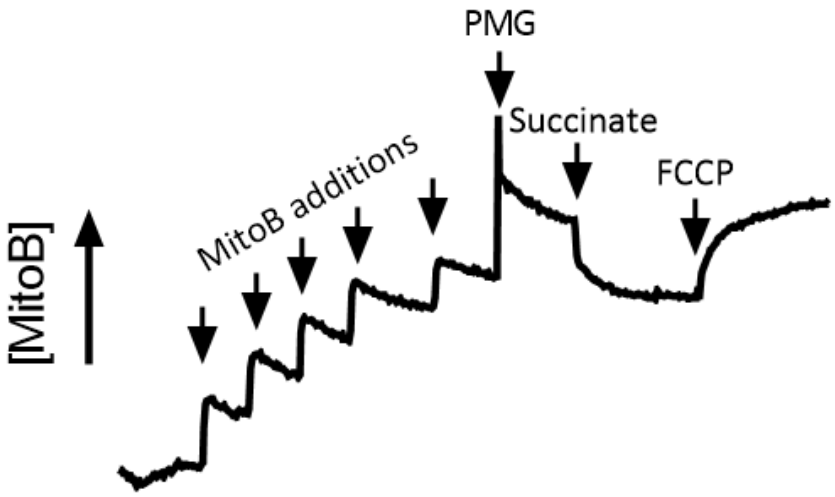

Figure S1. MitoB uptake detected with ion-selective electrode specific for detection of TPP^+ in isolated liver mitochondria of sculpin *Artedius lateralis*. Sequential additions of MitoB was followed by addition of complex I substrates (pyruvate, malate, and glutamate; PMG), complex II substrate (succinate), and uncoupler carbonyl cyanide 4-(trifluoromethoxy)phenylhydrazone (FCCP). See methods section for details.

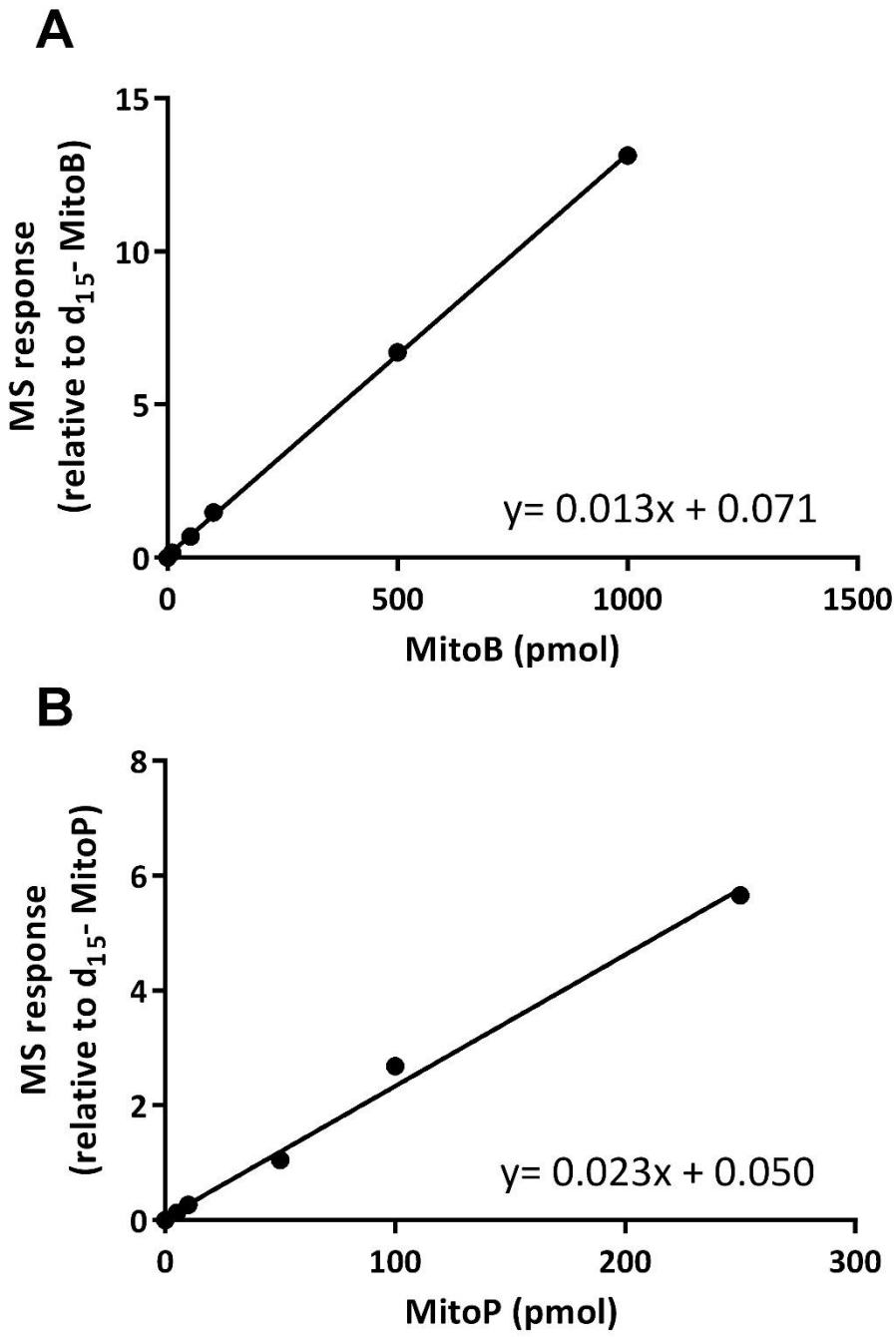

Figure S2. MitoB and MitoP standard curves for LC-MS/MS

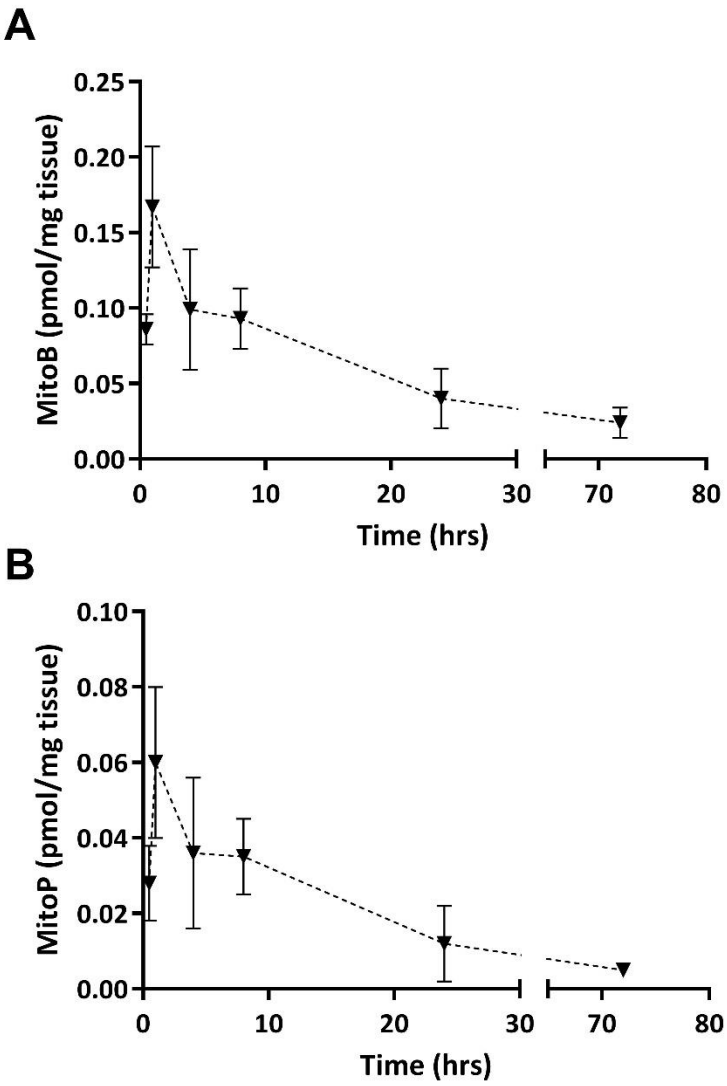

Figure S3. White muscle MitoB (top figure), converted MitoP (middle), and MitoP/MitoB (bottom) over 72hr post-injection in normoxic resting *O. maculosus*.

Tissue	Normoxia	Hypoxia	Hypoxia Recovery	Normoxia	Hyperoxia	Hyperoxia Recovery
			Oligocottus maculosus			
Brain	35.71 ± 3.28^{a}	126.88 ± 39.87^{b}	56.73 ± 9.69^{ab}	34.51 ± 3.24^{a}	141.40 ± 30.71^{b}	83.04 ± 21.29^{ab}
Liver	30.20 ± 4.49^{a}	41.26 ± 11.38^{a}	47.41 ± 4.15^{a}	38.52 ± 11.65^{a}	47.72 ± 9.76^{a}	27.15 ± 6.40^{a}
Gill	102.79 ± 14.78^{a}	96.17 ± 15.60^{a}	137.42 ± 7.19^{a}	96.81 ± 18.71^{a}	105.45 ± 31.53^{a}	107.38 ± 25.35^{a}
			Scorpaenichthys marmoratus			
Brain	74.62 ± 15.73^{a}	58.10 ± 9.19^{a}	46.89 ± 5.40^{a}	63.79 ± 13.26^{a}	35.81 ± 10.72^{a}	45.28 ± 9.96^{a}
Liver	27.85 ± 7.29^{a}	18.60 ± 6.51^{a}	36.43 ± 7.76^{a}	31.10 ± 5.55^{a}	53.19 ± 17.47^{a}	54.51 ± 14.39^{a}
Gill	54.32 ± 6.57^{a}	142.78 ± 31.56^{a}	130.60 ± 27.38^{a}	59.43 ± 10.53^{a}	114.94 ± 42.83^{a}	35.65 ± 4.03^{a}

Table S1. TBARS (in pmol/mg protein) to 3.5 kPa hypoxia-recovery and 64.0 kPa hyperoxia-recovery. One way ANOVA was used to analyse for each tissue the effect of hypoxia -recovery on TBARS .

Tissue	Normoxia	Hypoxia	Hypoxia Recovery	Normoxia	Hyperoxia	Hyperoxia Recovery
			Oligocottus maculosus			
Brain	14.40 ± 0.96[a]	17.00 ± 4.60[a]	12.60 ± 1.28[a]	14.2 ± 0.98[a]	18.00 ± 1.56[a]	17.00 ± 1.92[a]
Liver	167.80 ± 32.80[a]	54.80 ± 22.00[b]	120.20 ± 27.00[ab]	191.00 ± 24.20[a]	156.80 ± 37.80[a]	106.2 ± 15.40[a]
Gill	21.80 ± 1.66[a]	21.60 ± 1.42[a]	23.4 ± 0.60[a]	21.80 ± 3.40[a]	21.60 ± 0.98[a]	22.20 ± 2.80[a]
			Scorpaenichthys marmoratus			
Brain	15.00 ± 0.76[a]	15.40 ± 1.24[a]	17.40 ± 1.10[a]	17.60 ± 2.40[a]	13.80 ± 1.12[a]	17.20 ± 3.00[a]
Liver	109.60 ± 3.40[a]	84.80 ± 16.40[a]	173.20 ± 39.80[a]	119.80 ± 22.80[a]	263.20 ± 57.20[a]	201.60 ± 38.80[a]
Gill	23.20 ± 0.50[a]	24.40 ± 3.00[a]	28.20 ± 5.40[a]	26.60 ± 8.20[a]	22.20 ± 3.40[a]	27.00 ± 0.50[a]

Table S2 TOSC levels (expressed in μmole H_2O_2/min/mg protein) to 3.5 kPa hypoxia-recovery and 64.0 kPa hyperoxia-recovery. One way ANOVA was used to analyse the effect of hypoxia -recovery on TBARS in each tissue.

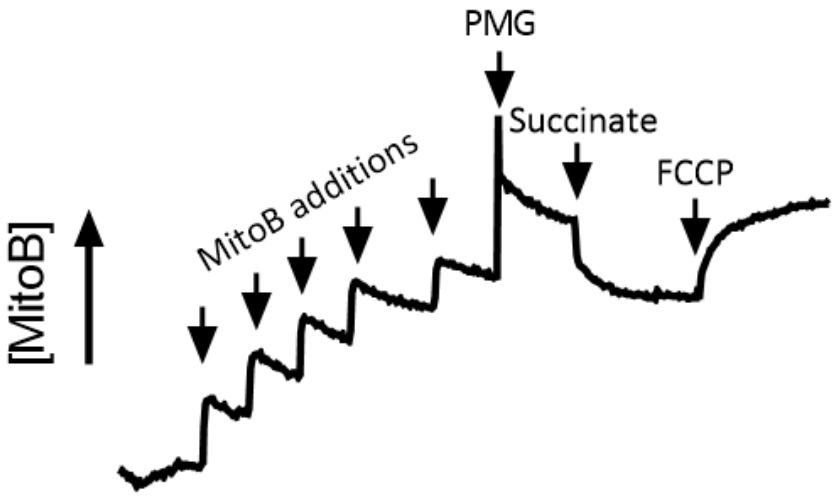

Figure S1. MitoB uptake detected with ion-selective electrode specific for detection of TPP^+ in isolated liver mitochondria of sculpin *Artedius lateralis*. Sequential additions of MitoB was followed by addition of complex I substrates (pyruvate, malate, and glutamate; PMG), complex II substrate (succinate), and uncoupler carbonyl cyanide 4-(trifluoromethoxy)phenylhydrazone (FCCP). See methods section for details.

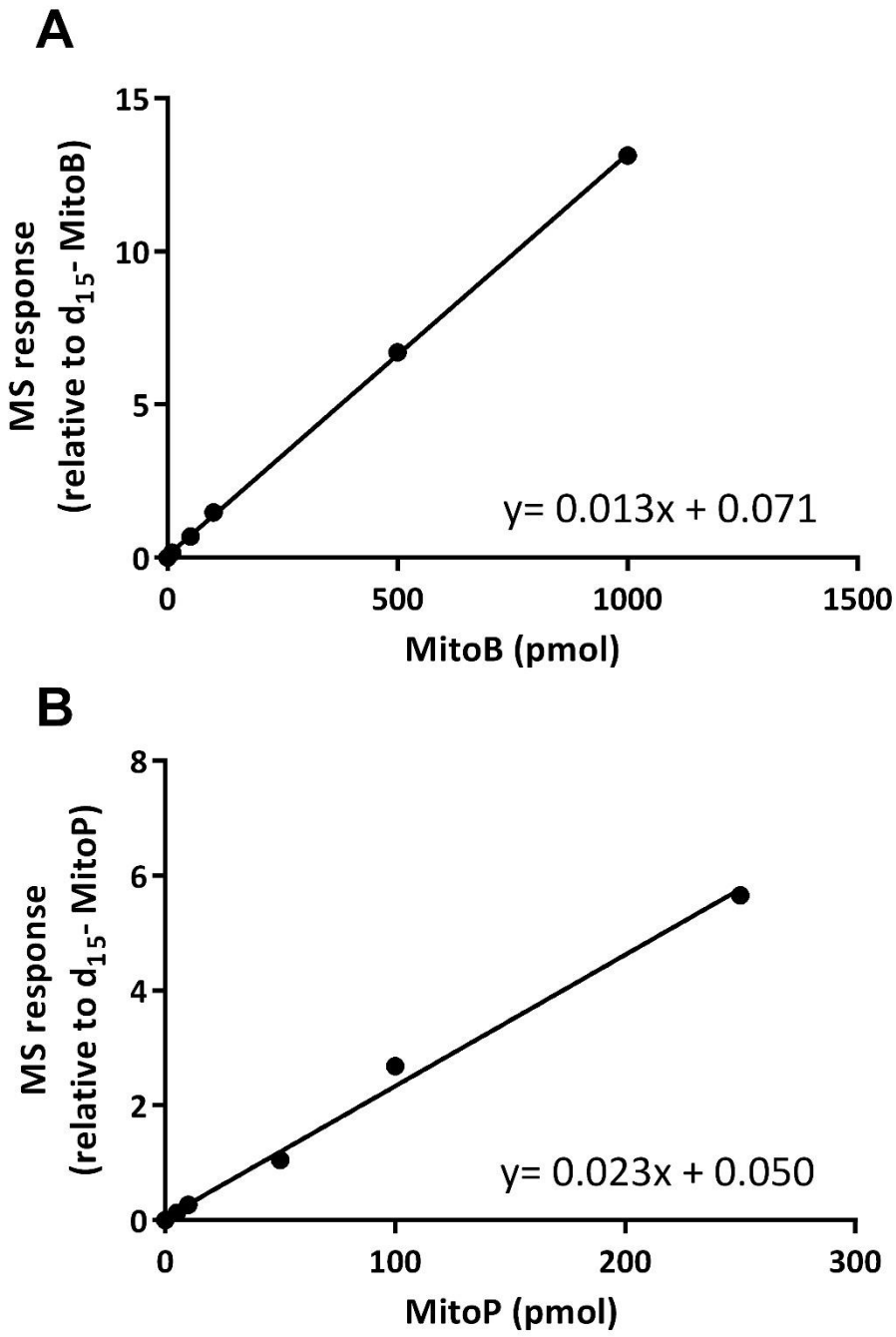

Figure S2. MitoB and MitoP standard curves for LC-MS/MS

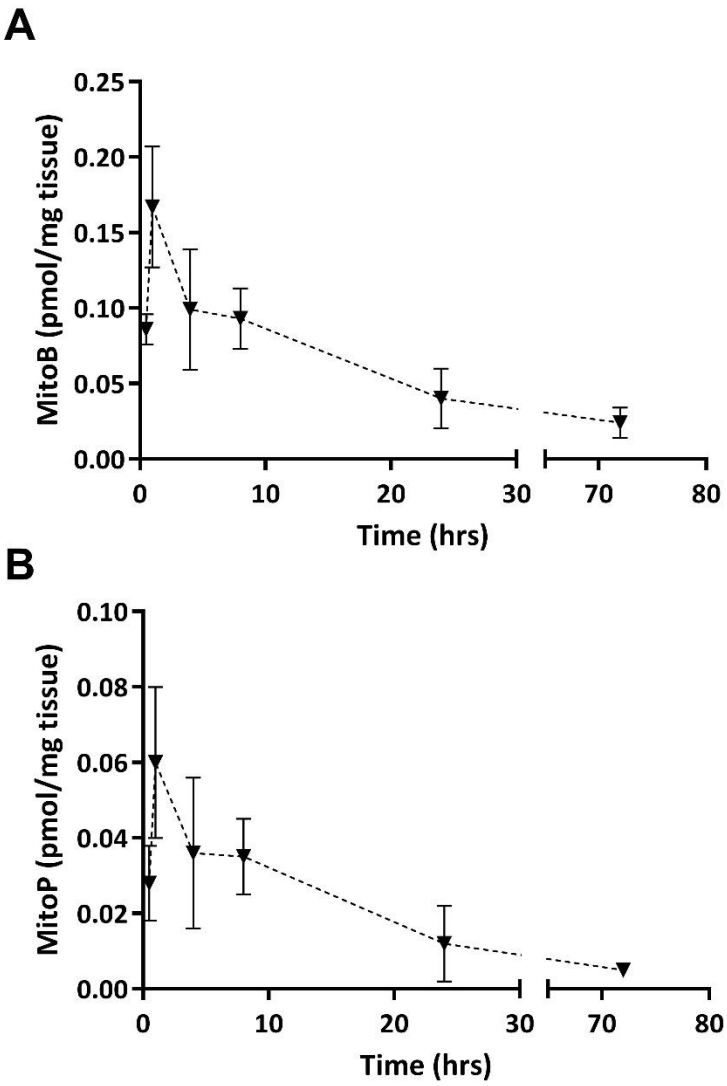

Figure S3. White muscle MitoB (top figure), converted MitoP (middle), and MitoP/MitoB (bottom) over 72hr post-injection in normoxic resting *O. maculosus*.

Tissue	Normoxia	Hypoxia	Hypoxia Recovery	Normoxia	Hyperoxia	Hyperoxia Recovery
			Oligocottus maculosus			
Brain	35.71 ± 3.28^{a}	126.88 ± 39.87^{b}	56.73 ± 9.69^{ab}	34.51 ± 3.24^{a}	141.40 ± 30.71^{b}	83.04 ± 21.29^{ab}
Liver	30.20 ± 4.49^{a}	41.26 ± 11.38^{a}	47.41 ± 4.15^{a}	38.52 ± 11.65^{a}	47.72 ± 9.76^{a}	27.15 ± 6.40^{a}
Gill	102.79 ± 14.78^{a}	96.17 ± 15.60^{a}	137.42 ± 7.19^{a}	96.81 ± 18.71^{a}	105.45 ± 31.53^{a}	107.38 ± 25.35^{a}
			Scorpaenichthys marmoratus			
Brain	74.62 ± 15.73^{a}	58.10 ± 9.19^{a}	46.89 ± 5.40^{a}	63.79 ± 13.26^{a}	35.81 ± 10.72^{a}	45.28 ± 9.96^{a}
Liver	27.85 ± 7.29^{a}	18.60 ± 6.51^{a}	36.43 ± 7.76^{a}	31.10 ± 5.55^{a}	53.19 ± 17.47^{a}	54.51 ± 14.39^{a}
Gill	54.32 ± 6.57^{a}	142.78 ± 31.56^{a}	130.60 ± 27.38^{a}	59.43 ± 10.53^{a}	114.94 ± 42.83^{a}	35.65 ± 4.03^{a}

Table S1. TBARS (in pmol/mg protein) to 3.5 kPa hypoxia-recovery and 64.0 kPa hyperoxia-recovery. One way ANOVA was used to analyse for each tissue the effect of hypoxia -recovery on TBARS .

Tissue	Normoxia	Hypoxia	Hypoxia Recovery	Normoxia	Hyperoxia	Hyperoxia Recovery
			Oligocottus maculosus			
Brain	14.40 ± 0.96[a]	17.00 ± 4.60[a]	12.60 ± 1.28[a]	14.2 ± 0.98[a]	18.00 ± 1.56[a]	17.00 ± 1.92[a]
Liver	167.80 ± 32.80[a]	54.80 ± 22.00[b]	120.20 ± 27.00[ab]	191.00 ± 24.20[a]	156.80 ± 37.80[a]	106.2 ± 15.40[a]
Gill	21.80 ± 1.66[a]	21.60 ± 1.42[a]	23.4 ± 0.60[a]	21.80 ± 3.40[a]	21.60 ± 0.98[a]	22.20 ± 2.80[a]
			Scorpaenichthys marmoratus			
Brain	15.00 ± 0.76[a]	15.40 ± 1.24[a]	17.40 ± 1.10[a]	17.60 ± 2.40[a]	13.80 ± 1.12[a]	17.20 ± 3.00[a]
Liver	109.60 ± 3.40[a]	84.80 ± 16.40[a]	173.20 ± 39.80[a]	119.80 ± 22.80[a]	263.20 ± 57.20[a]	201.60 ± 38.80[a]
Gill	23.20 ± 0.50[a]	24.40 ± 3.00[a]	28.20 ± 5.40[a]	26.60 ± 8.20[a]	22.20 ± 3.40[a]	27.00 ± 0.50[a]

Table S2 TOSC levels (expressed in μmole H_2O_2/min/mg protein) to 3.5 kPa hypoxia-recovery and 64.0 kPa hyperoxia-recovery. One way ANOVA was used to analyse the effect of hypoxia -recovery on TBARS in each tissue.